Mixing of an Acoustically Pulsed Air Jet with a Confined Crossflow

P. J. Vermeulen,* Ching-Fatt Chin,† and Wai Keung Yu†
University of Calgary, Calgary, Alberta, Canada

Mean velocity and turbulence profiles, downstream of the jet orifice, in a 10 m/s crossflow have been measured over a range of Strouhal numbers and excitation powers for a jet/crossflow velocity ratio range of 1.3 to 4.6. This showed that acoustically exciting a jet flow causes significant increases in jet spread, penetration (up to 92% increase), and mixing. The jet mixing length was strongly reduced. Toroidal vortices were shown to be shedding from the jet orifice and produced profound changes in the jet structure. Increase of jet penetration and turbulence (hence mixing) began to saturate by about 80-W driving power, thus only small further gains were possible up to the maximum power used of 160 W. The jet turbulence and penetration data showed that the response appeared to be optimum at about a Strouhal number of 0.22. Overall, the jet mixing processes were significantly improved, in a controllable manner, by pulsating the jet flow.

Nomenclature

a = jet axis, point of maximum velocity
c = location on centerline in orifice exit plane
D = jet orifice diameter
F = function
f = driving frequency
H = tunnel height
j = approximate boundary of the jet zone
p_∞ = crossflow static pressure at $X/D = -3.66$
R_{ej} = Reynolds number of jet at the orifice
$R_{e\infty}$ = Reynolds number of crossflow based on hydraulic diameter
St = jet Strouhal number at the orifice $= fD/U_j$
sl = approximate position of maximum shear defining jet lower boundary
su = approximate position of maximum shear defining jet upper boundary
T_j = temperature of the jet flow at orifice exit plane
T_∞ = crossflow temperature at $X/D = -3.66$
U = local mean velocity in X-Y plane at a particular X location
U_e = jet velocity excitation pulsation amplitude, or pulsation strength, at the orifice exit plane center (unsteady flow)
U_j = steady jet velocity at the orifice exit plane center
U_{rms} = local rms value of fluctuating velocity (turbulence) in X-Y plane at a particular X location
U^0_{rms} = overall (average over H) turbulence in X-Y plane at a particular X location
ΔU^0_{rms} = change in overall turbulence, caused by acoustic excitation, in X-Y plane at a particular X location
U_∞ = average crossflow velocity at $X/D = -3.66$ cross section
v = approximate edge of core region of the toroidal vortices shedding from the orifice
$\dot{W}$ = power at acoustic driver
X, Y, Z = rectangular coordinates; see Fig. 1 for origin location
ρ_j = density of the jet flow at orifice exit plane
ρ_∞ = crossflow density at $X/D = -3.66$

Presented as Paper 88-3296 at the AIAA/ASME/SAE/ASEE 24th Joint Propulsion Conference, Boston, MA, July 11-13, 1988; received Jan. 17, 1989; revision received Sept. 20, 1989.

*Professor, Department of Mechanical Engineering. Member AIAA.
†Graduate Student, Department of Mechanical Engineering.

Introduction

MANY investigations have been made into the mixing behavior of free gaseous jets and of gaseous jets mixing with a confined crossflow. These studies, up to fairly recently, have always been concerned with steady jet flows. However, Crow and Champagne[1] indirectly showed that jet entrainment was significantly increased for a low level of acoustic pulsation of the jet. Other workers[2-4] subsequently studied excited jet flows and by indirect means showed that the entrainment rate was increased. Vermeulen et al.[5] appear to have made the first direct measurements of the entrainment rate of acoustically pulsed free air jets and showed that entrainment may be increased by up to 5.8 times for the fully developed jet region. The mixing of a pulsed jet is therefore also significantly increased. Because jet flow mixing is of fundamental importance to the performance of a gas turbine combustor, and in particular the mixing of an air jet with a confined crossflow, an experimental investigation into the mixing behavior of an acoustically pulsed air jet with a confined crossflow has therefore been undertaken. Such a study will elucidate the basic nature of the process and therefore provide the fundamental understanding for possible applications, for example, the recent experiments on acoustic control of dilution air mixing.[6,7] Also, some indication of the future potential of the technique may be established. It is believed that an investigation of this phenomenon has not been made before.

Experimental

Apparatus for Acoustically Pulsed Air Jets in a Confined Crossflow

Figure 1 shows the apparatus whereby air jets may be injected into a uniform confined crossflow. Multiple opposed jets may be studied (up to 5 each in the tunnel test-section floor and ceiling), but because of the desire to develop a basic understanding, only a single jet, from the center of the test-section floor, has so far been thoroughly investigated. The jets, for convenience, were pulsed by loudspeaker drivers of 200-W capacity via tubes connected at right angles with the jet tubes. The air flow was supplied by a 45-kW blower, and by means of valves some air may be diverted in order to provide the jet flows. An orifice resistance plate could be mounted downstream of the branches for the jet flows in order to assist in controlling the jet/crossflow velocity ratio. The jet flow and crossflow were essentially at the same temperature. Settling

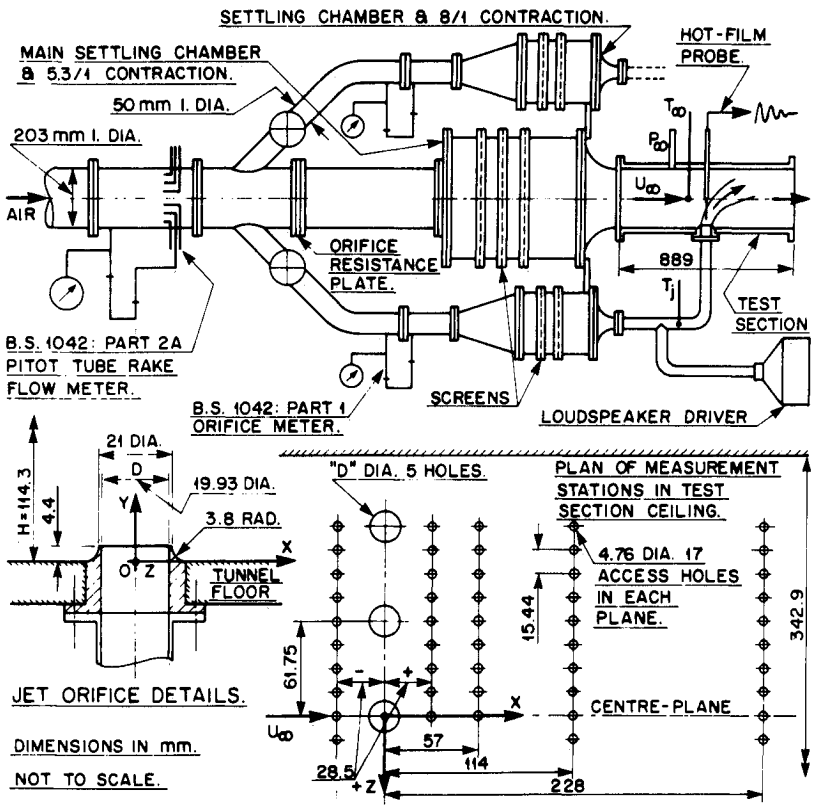

Fig. 1 Apparatus for acoustically pulsed air jets in a confined crossflow.

chambers with screens and an exit contraction were installed to produce good quality jets and crossflow. The jet flow branches were metered by means of standard sharp-edged orifice meters. The total mass flow from the blower was metered via two diametral rakes of 10 pitot tubes using the log-linear method recommended by British Standards BS: 1042 Part 2A.[8] The 114 × 343-mm (inside dimensions) rectangular cross-section test section had Perspex windows in all four walls. Through the ceiling a pattern of holes (plugged when not in use) (see Fig. 1) allowed mean velocity U and turbulence U_{rms} profiles to be measured by means of a hot-film anemometer calibrated in the standard manner. A traversing mechanism (not shown) permitted accurate vertical traverses to be made by the velocity probe. By these means the pulsed jet mixing was assessed by profile measurements made on several planes downstream of the jet orifice. The jet orifice (see Fig. 1) was lipped in similar manner to the dilution air holes of the combustor used in Ref. 6.

For safe operation of the acoustic source, power at the loudspeaker was measured by an ac voltmeter and ammeter. The power factor correction was ignored since similar tests had shown it to be small.[5] Acoustic excitation pulses the jet velocity at the orifice exit, which in turn excites the jet flow into wave motion developing into a train of toroidal vortices.[4] This jet pulsation velocity amplitude U_e at the orifice exit plane center was measured by a hot-film anemometer in a manner similar to Ref. 4.

The response of the excited jet flow system can be divided into the mechanical system of tubes plus loudspeaker and the jet flow. The frequencies of the strongest excitation of the jet are determined by the mechanical system response. These were established by means of dual channel fast Fourier transform (FFT) analysis at zero-flow conditions. They were then confirmed as the frequencies producing the strongest jet pulsation strength by manually changing the input frequency at the loudspeaker driver from about 50 to 1.2 kHz while keeping the input current constant at 2.0 A. The measurements were made over a range of jet velocities from 11 to 43 m/s, about that covered in the velocity profile measurements. A crossflow velocity, small enough to ensure minimal jet distortion in the orifice exit plane, was maintained so that the jet did not strike the tunnel ceiling. The results showed a strong resonance mode at 208 Hz and minor modes at 1020 and 1070 Hz, irrespective of jet velocity. Thus 208 Hz was selected as the optimum driving frequency and used in all tests. Furthermore, Vermeulen et al.[5] showed that the maximum increase in jet entrainment rate takes place at the frequency for best mechanical system response. The jet flow response depends on the Strouhal number St, and Refs. 4 and 5 showed this to be optimum at about 0.25 for a free jet, which should therefore have significance for this study.

The main factors affecting the mixing behavior are the jet velocity/crossflow velocity ratio U_j/U_∞, the jet relative pulsation strength U_e/U_j, the axial distance X downstream from the orifice exit plane, and the jet Strouhal number St. Measurements were made at $U_\infty = 10$ m/s, for a U_j/U_∞ range of 1.3 to 4.6 and for relative pulsation strengths U_e/U_j from 0 to 1.67. The downstream axial distance covered was from $X/D = 0$ to 11.44. The Strouhal number range of the tests was from 0.090 to 0.314. The jet orifice diameter bore was kept constant at 19.93 mm in order that the test results would relate to the performance of the combustor.[6] Also the crossflow velocity of 10 m/s, corresponding to the low end of this combustor's Mach number range of 0.03 to 0.07, was selected to ensure that the maximum jet velocity used could be effectively pulsed by the driver power available.

Apparatus Calibrations

The total mass-flow-rate, pitot tube flow meter was calibrated over the full operation range. During calibration, all of the air flow passed through the test section, and therefore this mass flow rate was referred to the reference velocity measured by a pitot tube-static tube pair at $X/D = -3.66$, $Y/H = 0.50$, and $Z/D = +4.78$ to avoid interference from the jet flow. Thus the test-section crossflow mass-flow-rate was

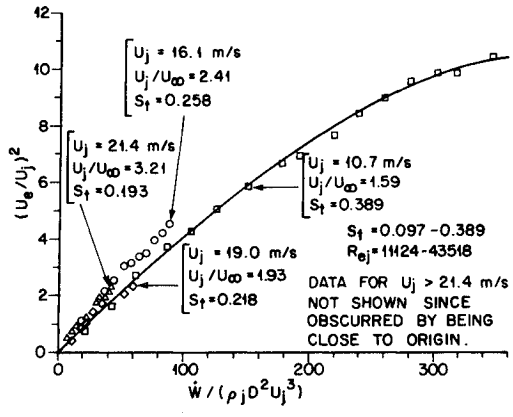

Fig. 2 Relative pulsation strength vs dimensionless driving power; 19.93-mm-diam orifice, 208 Hz.

conveniently calibrated (linearly) against density × velocity at the reference pitot-static tubes.

Measurements of mean axial velocity and turbulence level vertical profiles in the test section were obtained on transverse planes $X/D = -1.43$ (upstream), 5.72 and 11.44, for lateral positions $Z/D = 0$ (center plane), ± 3.10 and ± 6.20, for 1/4 and 1/1 of the maximum mass-flow-rate. This was for no jet flow, and the tunnel walls had been rendered flush by appropriate sealing plugs. All measured profiles behaved stably and were acceptably flat, indicating that no adverse flow conditions had occurred. The turbulence level U_{rms}/U_∞ on the tunnel center line at $X/D = -1.43$ for 1/4 mass-flow-rate (U_∞ = 15.1 m/s) was 2.8% and for 1/1 mass-flow-rate (U_∞ = 75.5 m/s) was 1.7%. An investigation was also undertaken to ascertain possible blockage effects at the reference pitot caused by the jet flow for "no-drive" and "with-drive" conditions. The measured mean velocity and turbulence level profiles at $X/D = -1.43$, and $Z/D = 0.0$, ± 3.1 showed no significant blockage effects, and hence the test-section crossflow calibration in terms of the reference pitot was not affected by the jet flow, even when acoustically excited.

The jet pulsation strength was calibrated at 208 Hz over a range of jet flow velocities from 10.7 to 42.7 m/s, with U_∞ from 6.7 to 10.3 m/s, respectively, and over the full driving power range 0–160 W (limited by amplifier distortion). Also the pulsation strength was measured for each individual velocity profile measurement test. The results are summarized in Fig. 2 using the correlation of Ref. 5. Interestingly, traversing the hot-film sensor vertically upward revealed the velocity-time distribution typical of a vortex core, for all the pulsating flows tested, and hence confirmed the presence of toroidal vortices.[4,6]

Experimental Results—Velocity and Turbulence Profiles

Figure 3 shows the structure of the jet crossflow corresponding to the typical mean velocity profiles on the center plane ($Z/D = 0$) of Fig. 4, at approximately the optimum Strouhal number, and for zero and medium excitation. The corresponding turbulence profiles are shown in Fig. 5. The turbulence profiles were a considerable aid in establishing the characteristic features of the jet in crossflow and therefore in constructing Fig. 3. Thus the maximum region in the mean velocity and turbulence profiles, between points *jj*, is the jet zone, which is composed of jet fluid as well as fluid entrained by shearing and mixing at the jet boundary. Beyond the upper point *j*, the crossflow becomes dominant. For the no-drive jet, it is common practice to take the point of maximum velocity *a* to be on the axis of the jet, which locus then defines the center plane jet trajectory. However, for with-drive conditions, the velocity profile is considerably broadened with uncertainty as to the position of the jet axis. The point *a* was therefore determined by reference to the "inflection" in the corresponding turbulence profile (compare the no-drive velocity and turbulence profiles at $X/D = 1.43$ of Figs. 4 and 5).

When interpreting the velocity profiles, it should be borne in mind that even though the hot-film sensor was aligned with its axis paralled to the Z direction, fluid velocities would be measured in the X-Y plane irrespective of direction. Also, components of velocities that are not aligned in the X-Y plane would be measured. This complicates interpretation of the measured profiles, particularly those measured in planes lateral to the center plane.

Test Results "without Acoustic Drive"

Referring to the no-drive profiles of Figs. 4 and 5, $X/D = 0.0$, the data is for an oblique traverse over half the jet flow and reveals mean velocity and turbulence profiles typical of fully developed pipe flow. The peak value of turbulence or maximum shear *su* at $X/D = 0.0$ in Fig. 5 defines the jet upper boundary, and the traverse at $X/D = 1.43$ reveals the maximum turbulence or shear *sl* associated with the jet lower boundary. From *sl* ($X/D = 1.43$), the turbulence reduces to the inflection at point *a* before decreasing again at *su*. The disappearance of the minimum present in the initial turbulence profile at point *c* ($X/D = 0.0$) is due to masking by increasing turbulence caused by entrainment and mixing. Thus the turbulence profile *sl* to *su* represents the last vestiges of the jet's initial distribution. The absence of a maximum at *su* is due to the reduction in shear (and masking) caused by the crossflow

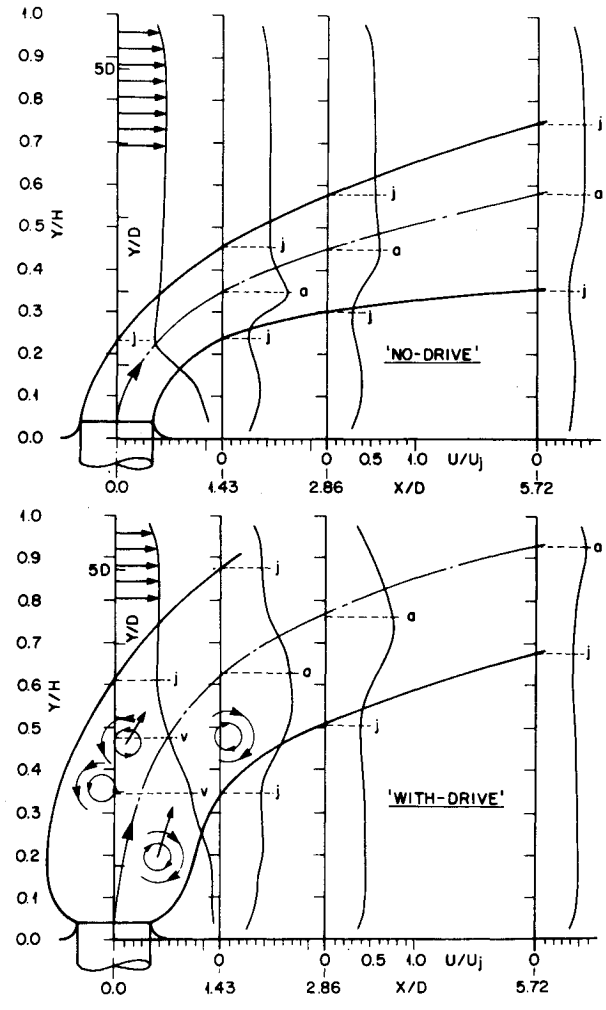

Fig. 3 Structure of center plane jet crossflow corresponding to the velocity profiles of Fig. 4; St = 0.218, U_e/U_j = 1.18, 75.3 W.

reducing the relative velocity between the jet flow and the surrounding fluid. The zone from $Y/H = 0$ to the first point j in Figs. 4 and 5 is a complicated entrainment-wake region downstream of the jet. These features are consistent with published work.[9]

The mean velocity and turbulence profiles at $X/D \geq 1.43$ (no-drive) show peak values were decreased, the jet depth jj increased, and the profiles became more uniform as turbulent entrainment and mixing with the crossflow fluid proceeded. By $X/D = 11.44$, the mean velocity and turbulence profiles were fairly uniform indicating the mixing was largely completed. The jet trajectories, from all of the data, clearly showed that the jet penetration increased with velocity ratio U_j/U_∞.

Lateral mean velocity profile measurements (no-drive) showed that the jet axis coincided with the center plane. Symmetry about the center plane was good, and as U_j/U_∞ was increased, jet spreading (width in Z direction) was found to be greater. All of the lateral profiles exhibited features similar to those of the corresponding center plane profiles.

Test Results "with Acoustic Drive"

Consider the center plane mean velocity distributions of Fig. 4. At the location $X/D = 0.0$, $Y/H = 0.04$ (center of orifice exit plane), a significant increase in mean velocity was detected (point c), even though the mass-flow-rate to the jet was kept constant. This is considered to be due to the large pulsation strength ($U_e/U_j > 1$) causing reverse flow and hence a rectified signal,[10] which is then averaged by the anemometer-linearizer output to give an apparent increase in velocity. Of course, this is an ambiguous situation, but it serves to warn of the presence of reverse flow with consequently some ingestion of crossflow fluid into the orifice, which is then expelled on the positive pulse.[11] Furthermore, when $U_e/U_j < 1$, this apparent increase in velocity disappeared, i.e., there was no reverse flow.

The acoustic drive increases jet penetration, as shown by the displacement of point a in Figs. 4 and 5. This is also reflected in the displacement of the jet zone jj. The shear regions sl and su can still be identified from Fig. 5 and by comparing Figs. 4 and 5 at $X/D = 0.0$, a linear region vv can be recognized. This

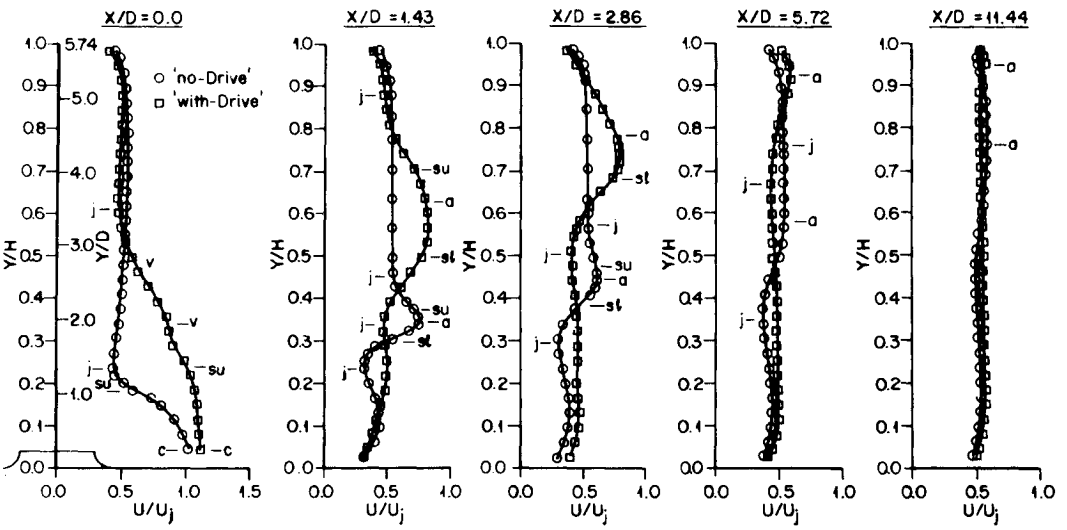

Fig. 4 Mean velocity profiles on center plane for zero and medium (75.3 W) powers, approximate optimum $St = 0.218$; 19.93-mm-diam orifice, $U_j = 19.0$ m/s, $U_j/U_\infty = 1.93$, $U_e/U_j = 1.18$, 208 Hz, $R_{ej} = 20294$, $R_{e\infty} = 83567$, $\rho_j = 1.008$ kg/m^3, $\rho_\infty = 0.966$ kg/m^3.

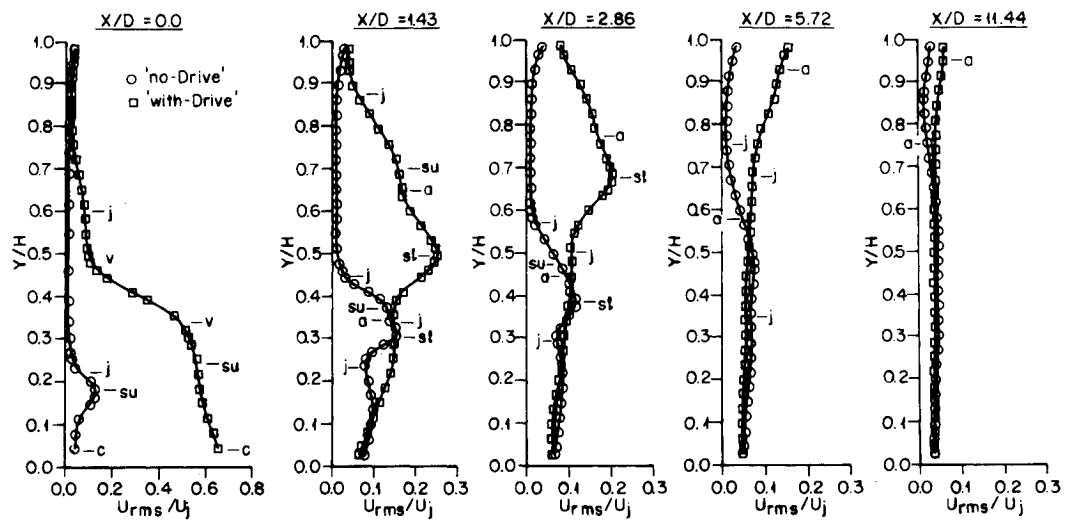

Fig. 5 Turbulence profiles on center plane for zero and medium (75.3 W) powers, approximate optimum $St = 0.218$; 19.93-mm-diam orifice, $U_j = 19.0$ m/s, $U_j/U_\infty = 1.93$, $U_e/U_j = 1.18$, 208 Hz.

is the core region[12] of the toroidal vortices shedding from the orifice, and the zone *su-v-v-j* is associated with toroidal vortex mixing and entrainment and may represent a true increase in mean velocity. Because of the ambiguity in mean velocity measurement, particularly near the orifice, the entire jet zone *c-su-v-v-j* is perhaps best thought of as a zone of agitation and mixing.

Figures 3 and 4 show acoustic excitation produces significant changes in the velocity profiles (increasing with pulsation strength), in particular, the jet zone *jj* has greater depth than for the no-drive case, and the wake region has undergone strong modification.

By $X/D = 5.72$, in Fig. 4, the velocity profile is nearly uniform across the duct for the excited case indicating that a more uniformly mixed state is reached sooner. It should be realized that from $X/D = 1.43$ and onward there was no experimental evidence of reverse flow (except perhaps in the vortex core region), and hence data interpretation is not complicated by such considerations. The increased velocity magnitude and jet flow area at large U_e/U_j implies a substantial increase in entrainment.

Examining next the center plane turbulence profiles of Fig. 5, strong changes produced by the acoustic excitation are immediately obvious. For instance the orifice centerline turbulence (point *c*) is greatly increased. However, the pulsation amplitude U_e was found to be the same as $\sqrt{2}\ U_{\text{rms}}$ at point *c* for $U_e/U_j < 1$ for all the with-drive tests as they should be for sinusoidal pulsations. Also for $U_e/U_j > 1$, the pulsation velocity was less sinusoidal,[4] and rectification of the signal was performed by the hot-film sensor; thus $\sqrt{2}U_{\text{rms}}$ was smaller then U_e (see Fig. 5). Hence the "turbulence" at point *c* (with-drive) is not true turbulence but the rms value of the pulsation velocity, with distortion effects when $U_e/U_j > 1$. The whole jet zone *c-su-v-v-j* is best thought of as pseudoturbulence, or agitation, being largely composed of pulsating flow in the core region[12] *c-su* and induced pulsating flow due to traveling toroidal vortices in the outer region *su-v-v-j*. The zone is considerably more vigorous than for the no-drive condition.

As Fig. 5 shows, there is rapid decay of the velocity pulsations and perhaps toroidal vortices. In fact the typical velocity structure of the vortex core could not be detected at $X/D = 2.86$. The more rapid decay of the toroidal vortices here, than for the pulsating free jet,[12] is presumed to be due to the shearing action of the crossflow fluid which opposes the rotation of the toroidal vortices. Thus from $X/D = 1.43$ onward U_{rms} is a better indication of true turbulence, and the toroidal vortices are degenerating into large-scale turbulence structures. Entrainment by the jet is taking place from the crossflow and augmented by the acoustic drive[5]; therefore the increased turbulence profile, both in extent and magnitude, indicates that acoustic excitation has improved the entrainment and mixing by the jet at $X/D \geq 1.43$.

Temperature profiles for cold steady jets in a hot crossflow[13] show that in the wake region beneath the jet ($X/D = 1.43$ and 2.86), some jet fluid and crossflow fluid mix. It is assumed that this continues for a pulsed jet, and therefore the much increased and modified wake region represents a vigorous mixing zone of some jet and crossflow fluid. Thus the acoustically increased zone of jet and wake represents a more greatly improved mixing of jet and crossflow fluid than for the no-drive situation.

By $X/D = 5.72$ (see Fig. 5) the turbulence has decayed considerably, but now the acoustically enhanced jet affects, fairly uniformly, the whole tunnel flow depth (penetration is complete), and taken in conjunction with the almost uniform velocity profile of Fig. 4, suggests that the excited jet is well mixed. The length to achieve full mixing has therefore been shortened from about $X/D = 11.44$ to 5.72 by the acoustic drive and is even shorter at greater powers.

Lateral mean velocity profile measurements showed that acoustic excitation appeared to have produced little change in jet width but significantly increased the jet depth and hence cross-sectional area. The characteristic kidney-shaped cross section[9] for no-drive was transformed to an oval cross section ($1.43 < X/D < 2.86$) except for the smallest U_j/U_∞ value tested, and even here the kidney shape was less pronounced. This suggests that acoustic drive has produced strong flowfield modification, perhaps worthy of a detailed flow visualization study. The profile features and changes with downstream distance were consistent with those shown by the center plane results.

The lateral turbulence profiles with-drive showed overall characteristic features consistent with those displayed by the lateral mean velocity profiles.

Discussion

Velocity Pulsation Strength

Provided the crossflow velocity is not too large, the jet behavior close to the orifice exit plane should essentially be that of a free jet, and therefore the result of dimensional analysis and experimentation from Ref. 5 should apply, i.e.,

$$\left(\frac{U_e}{U_j}\right)^2 = F\left(\frac{\dot{W}}{\rho_j D^2 U_j^3}\right) \tag{1}$$

Plotting the data in this fashion (see Fig. 2) indeed shows a good correlation, but the relationship is not linear, whereas the Ref. 5 case was linear because of the restricted data range considered. Nonlinearity may be due in part to strong reverse flow at the orifice exit causing unsymmetrical flow behavior[11] with increased losses and reduced U_e.

Because the Reynolds number and Strouhal number range of the data are large, and correlation of effects is erratic, the modest separation of the low U_j/U_∞ data is presumed to be due to the influence of the crossflow velocity[14] affecting the measurement of U_e. Nevertheless the correlation is very useful allowing easy experimental control via simple measurement of driver voltage and current. However, it is not universal since changing the driving system will change the calibration.

Jet Penetration

From the jet trajectory data, the increased jet penetration with relative pulsation strength U_e/U_j can be obtained. This is presented in Fig. 6 for various downstream locations, at about the optimum Strouhal number, as a function of $(U_e/U_j)^2$, which is approximately proportional to driving power. The increase of penetration with the acoustic drive is clearly shown, as is the suppression of penetration by the tunnel ceiling for $X/D = 5.72$ and 11.44. Interference by the tunnel ceiling appears to be minimal at $X/D = 1.43$ and 2.86. Thus at these locations, the increase of penetration starts to saturate

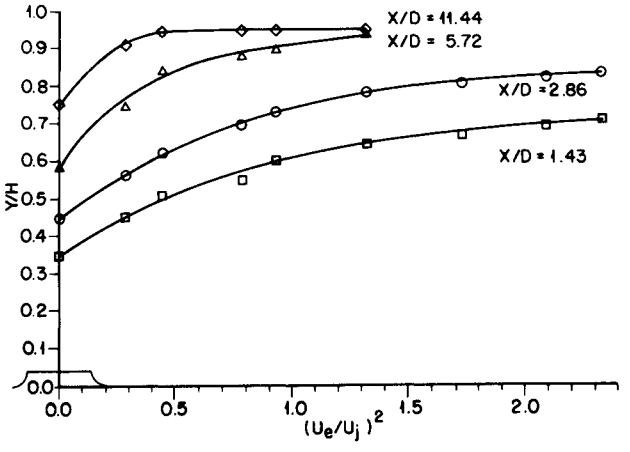

Fig. 6 Center plane jet penetration vs relative pulsation strength, approximate optimum $St = 0.218$; 19.93-mm-diam orifice; see Fig. 4 for other data.

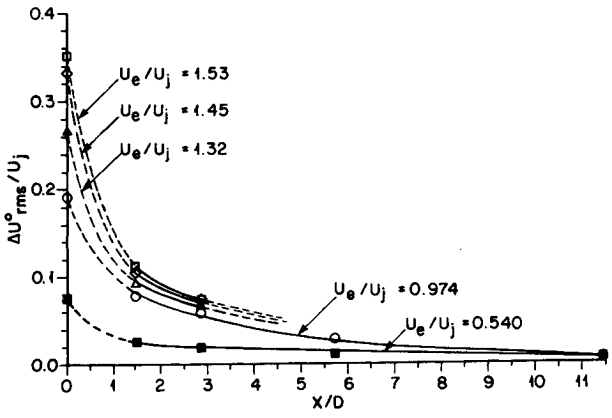

Fig. 7 Relative change in overall turbulence by acoustic excitation vs downstream distance, approximate optimum $St = 0.218$; 19.93-mm-diam orifice; see Fig. 4 for other data.

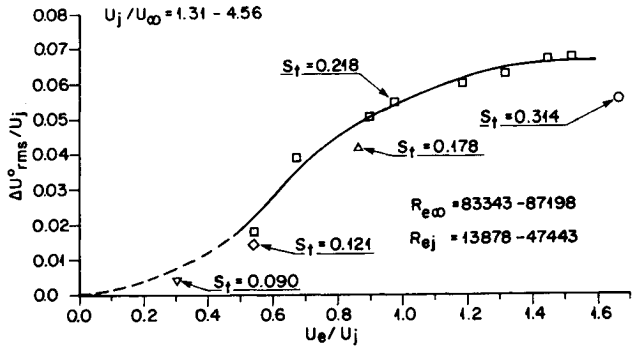

Fig. 8 Relative change in overall turbulence vs relative pulsation strength showing Strouhal number effect; 19.93-mm-diam orifice, $X/D = 2.86$, 208 Hz.

by about $(U_e/U_j)^2 = 1.5$ (about 80 W), and hence further gains in penetration by increasing the excitation are small. The maximum increase of penetration is therefore about 92% at $X/D = 2.86$. This behavior is consistent with the findings of Refs. 4 and 5, which speculated that the saturation may be due to the excitation of the toroidal vibration mode of the toroidal vortices shedding from the orifice.

Turbulence

The turbulence measurements may be presented in an overall way by calculating the average or overall turbulence U^0_{rms} for a given turbulence profile. This was done for profiles with and without acoustic excitation, and then the difference was taken to define ΔU^0_{rms}. Thus this parameter represents the average or overall increase in turbulence due to acoustic excitation. Also the turbulence of the crossflow is eliminated. Figure 7 presents this information, in dimensionless form, showing the effect of pulsation strength at the approximate optimum Strouhal number, and Fig. 8 shows the effect of Strouhal number for all the available data at $X/D = 2.86$, the location where jet response should be well established.

Acoustic excitation increases U^0_{rms} by more than three times at $X/D = 1.43$ for $St = 0.218$, discounting the greater change at $X/D = 0.0$ since this is largely pseudoturbulence. The ΔU^0_{rms} represents greater mixing, due to acoustic excitation, over the downstream range, and therefore the length to achieve a given state is shortened by excitation. The decay of ΔU^0_{rms} (see Fig. 7) indicates that U^0_{rms} decays faster (with X/D) when excited than for no-drive. Thus the greater turbulence momentum due to excitation decays faster than for the no-drive case. This must indicate that mixing with the lower momentum crossflow has been increased, with increase of entrainment mass-flow-rate in agreement with Ref. 5, i.e., mixing has been improved by acoustic excitation.

Figure 8 demonstrates that the curve for $St = 0.218$ forms an upper boundary for the available data and strongly suggests that this is closely the optimum condition. Crow and Champagne[1] used a similar method for a free jet except that they used the centerline turbulence of the jet to deduce an optimum Strouhal number of 0.30. This was not used here because of the uncertainty in defining the jet axis and because the combined response of the jet-crossflow interaction from a mixing viewpoint was the main interest. Examining the jet penetration data also revealed that data at $St = 0.218$ formed an upper bound, although not so clearly as Fig. 8. The response is therefore optimum at about 0.22 Strouhal number and is in agreement with $St = 0.25$ found for the optimum entrainment rate and mixing by a free jet.[4,5]

It is of significance to notice that ΔU^0_{rms} and also U^0_{rms} begin to saturate with increase of pulsation strength when $U_e/U_j = 1.2$ (75 W). Therefore turbulence may still be increased somewhat further (hence mixing) by increasing U_e/U_j up to the maximum power used of 160 W, although the limit is about reached. Vermeulen et al.[5] found a similar situation for the increase in entrainment mass-flow-rate.

Conclusions

The experimental results showed that acoustically exciting a jet flow in a confined crossflow produced strong changes in the mean velocity and turbulence profiles. This resulted in significant increases in jet spread, penetration (up to 92% increase), and mixing.The jet mixing length was strongly reduced. Toroidal vortices were shown to be shedding from the jet orifice and produced profound changes in the jet structure. In particular, the characteristic kidney-shaped cross section for no-drive was transformed to an oval cross section. Increase of jet penetration and turbulence (hence mixing) begin to saturate by about 80-W driving power, thus only small further gains were possible up to the maximum power used of 160 W. The jet turbulence and penetration data showed that the response appeared to be optimum at about a Strouhal number of 0.22. Overall, the jet mixing processes were significantly improved, in a controllable manner, by pulsating the jet flow.

Acknowledgments

The work was supported financially by the Natural Sciences and Engineering Research Council of Canada under Grant A7801. The authors are indebted to W. A. Anson, Chief Technical Supervisor; R. Bechtold, Machine Shop Supervisor; and particularly to technicians W. Crews and P. Halkett for their careful work in the building and operation of the test rig.

References

[1]Crow, S. C., and Champagne, F. H., "Orderly Structure in Jet Turbulence," *Journal of Fluid Mechanics*, Vol. 48, Part 3, Aug. 1971, pp.547-591.

[2]Binder, G., and Favre-Marinet, M., "Mixing Improvement in Pulsating Turbulent Jets," *ASME Symposium on Fluid Mechanics of Mixing*, Georgia Inst. of Technology, Atlanta, GA, June 1973, pp. 167-172.

[3]Hill, W. G., and Greene, P. R., "Increased Turbulent Jet Mixing Rates Obtained by Self-Excited Acoustic Oscillations," *Transactions of the ASME, Journal of Fluids Engineering*, Vol. 99, No. 3, Sept. 1977, pp. 520-525.

[4]Vemeulen, P. J., and Yu, W. K., "An Experimental Study of the Mixing by an Acoustically Pulsed Axisymmetrical Air-Jet," *International Journal of Turbo & Jet-Engines*, Vol. 4, Nos. 3-4, 1987, pp. 225-237.

[5]Vermeulen, P. J., Ramesh, V., and Yu, W. K. "Measurements of Entrainment by Acoustically Pulsed Axisymmetric Air Jets," *Transactions of the ASME, Journal of Engineering for Gas Turbines and Power*, Vol. 108, No. 3, July 1986, pp. 479-484.

[6]Vermeulen, P. J., Odgers, J., and Ramesh, V., "Acoustic Control of Dilution-Air Mixing in a Gas Turbine Combustor," *Transactions of the ASME, Journal of Engineering for Power*, Vol. 104, No. 4, Oct. 1982, pp. 844-852.

[7]Vermeulen, P. J., Odgers, J., and Ramesh, V., "Full Load Operation of a Gas Turbine Combustor with Acoustically Controlled Dilution-Air Mixing," *International Journal of Turbo & Jet-Engines*, Vol. 4, Nos. 1-2, 1987, pp. 139-147.

[8]B.S. 1042: Part 2A: 1973, "Methods for the Measurement of Fluid Flow in Pipes. Part 2. Pitot Tubes. 2A. Class A Accuracy," British Standards Institution, London, 1973.

[9]Moussa, Z. M., Trischka, J. W., and Eskinazi, S., "The Near Field in the Mixing of a Round Jet with a Cross Stream," *Journal of Fluid Mechanics*, Vol. 80, Part 1, April 1977, pp. 49-80.

[10]Yu, W. K., "An Experimental Study of the Mixing Behavior of Acoustically Pulsed Air Jets," M. S. Thesis, Dept. of Mechanical Engineering, The Univ. of Calgary, Calgary, Alberta, Canada, July 1985.

[11]Disselhorst, J. H. M., and Van Wijngaarden, L., "Flow in the Exit of Open Pipes During Acoustic Resonance," *Journal of Fluid Mechanics*, Vol. 99, Part 2, July 1980, pp. 293-319.

[12]Vermeulen, P. J., and Odgers, J., "Acoustic Control of the Exit Plane Thermodynamic State of a Combustor," American Society of Mechanical Engineers, New York, Paper 79-GT-180, March 1979.

[13]Holdeman, J. D., and Walker, R. E., "Mixing of a Row of Jets with a Confined Crossflow," *AIAA Journal*, Vol. 15, No. 2, 1977, pp. 243-249.

[14]Andreopoulos, J., and Rodi, W., "Experimental Investigation of Jets in a Crossflow," *Journal of Fluid Mechanics*, Vol. 138, Jan. 1984, pp. 93-127.